Journal of the European Ceramic Society 21 (2001) 1055–1060

www.elsevier.com/locate/jeurceramsoc

Compressive creep of polycrystalline $ZrSiO_4$

K.C. Goretta [a,*], T.A. Cruse [a], R.E. Koritala [a], J.L. Routbort [a], J.J. Mélendez-Martínez [b], A.R. de Arellano-López [b]

[a] *Energy Technology Division, Argonne National Laboratory, Argonne, IL 60439-4838, USA*
[b] *Departmente de Fisica de la Materia Condensada, Universidad de Sevilla, PO Box 1065, 41080 Sevilla, Spain*

Received 20 July 2000; received in revised form 17 October 2000; accepted 12 November 2000

Abstract

Polycrystalline $ZrSiO_4$ ceramics were prepared from commercial powder. Silicate-based glass phase was observed at multiple-grain junctions. Compressive creep tests were conducted in Ar at 1197–1400°C. For stresses of ≈1–120 MPa, steady-state creep occurred by diffusional flow. For stresses of >3 MPa, the steady-state strain rate $\dot{\varepsilon}$ could be expressed as

$$\dot{\varepsilon} = A\sigma^{1.1\pm0.1}\exp - [(470 \pm 40 \text{ kJ/mol})/RT],$$

where A is a constant, σ the steady-state stress, R the gas constant, and T the absolute temperature. At 1400°C and 1 MPa, an increase in the value of n was observed. Electron microscopy revealed no deformation-induced change in the microstructures of any of the specimens, which is consistent with creep by diffusion-controlled grain-boundary sliding. Comparison with literature data indicated that volume diffusion of oxygen controlled the creep rate.

Keywords: Compressive creep; Creep; Grain boundary sliding; $ZrSiO_4$

1. Introduction

$ZrSiO_4$-based ceramics are used in refractories[1,2] and are being considered for containment of nuclear-weapons wastes.[3] $ZrSiO_4$ exhibits excellent high-temperature stability,[1–6] and is, therefore, also being considered as a matrix for various ceramic composites.[7–11] Few data have been published on the mechanical performance of $ZrSiO_4$, despite its manifold potential uses.[7–11]

Carbonneau et al. studied creep and fracture of $ZrSiO_4$ at temperatures of 1010–1240°C.[12,13] Their specimens, which contained ≈9% glass phase, were tested in flexure at stresses of ≈18–70 MPa. Cavitational damage was observed and stress exponents n were 2–3. An activation energy Q for an apparent steady-state response was estimated from a plot of $\dot{\varepsilon}/A\sigma^n$ vs. $1/T$, where $\dot{\varepsilon}$ is the steady-state strain rate, A a constant, σ the steady-state stress, and T the absolute temperature. The value calculated, 625 kJ/mol, is typical of that for many structural ceramics;[14] however, exactly what this value reflects is not clear. Stress exponents of 2–3 do not correspond to any standard steady-state creep mechanism, and the effects on tensile deformation of such large concentrations of glass are not clear. It is possible, for example, that the $ZrSiO_4$ deformation proceeded by a mechanism such as dissolution and reprecipitation within the glass phase, rather than by a conventional diffusional mechanism. If so, the value of Q would reflect the heat of solution rather than motion within the solid phase of the slowest-diffusing species.[15]

The goals of this study were to produce $ZrSiO_4$ specimens with essentially clean grain boundaries and then determine from creep tests the steady-state deformation mechanism and the values of n and Q. Compression tests were selected so that cavitional damage could be minimized.

2. Experimental details

2.1. Specimen preparation and characterization

$ZrSiO_4$ powders were obtained from Alfa Aesar (Ward Hill, MA). The particle size of the as-received

* Corresponding author.
E-mail address: goretta@anl.gov (K.C. Goretta).

0955-2219/01/$ - see front matter
PII: S0955-2219(00)00316-2

powder was ≈1.0 μm. After ball-milling with Y_2O_3-stabilized ZrO_2 grinding media for 72 h in isopropyl alcohol, the average particle size was reduced to 0.7 μm, with a surface area, as determined by BET analysis, of 11 m^2/g. X-ray diffraction indicated that the powder consisted of a single crystalline phase. Chemical analysis by inductively coupled plasma atomic emission spectroscopy (ICP-AES) revealed a moderate concentration of cation impurities (Table 1).

Specimens for creep testing were prepared by first cold-pressing dry powders in a cylindrical die. The resultant compacts were placed on ZrO_2 plates and sintered in air at 1550°C for 3–5 h. (Reports in the literature have indicated that $ZrSiO_4$ decomposes at 1540°C,[1,2,4] but that determination was based primarily on powders that contained ≈3% cation impurities. For purer powders, the decomposition has been reported to occur at or near 1676°C.[5,6])

Final specimens were ≈5.25 mm tall, ≈3.5 mm in diameter, and ≈99% dense. The density was determined from scanning electron microscopy (SEM) photomicrographs by measuring the porosity of polished specimens. A polished surface was thermally etched in air at 1475°C for 1 h to reveal the initial microstructure. SEM indicated an equiaxed grain structure, with an average grain size, as determined by a linear-intercept method,[16] of 1.2±0.2 μm; the largest grains were ≈5 μm in average dimension. Substantial etching of a glass phase appeared to have occurred (Fig. 1). Transmission electron microscopy (TEM) of foils polished and ion-thinned by conventional means supported the SEM observations. A SiO_2-based glass was confirmed to be present at triple junctions and pockets between more than three grains (Fig. 2). The grain boundaries were otherwise free of glass, to the scale of the observation; however, no high-resolution TEM was conducted. SEM and TEM observations indicated that the $ZrSiO_4$ specimens contained ≈5% glass.

2.2. Creep tests

The $ZrSiO_4$ specimens were compressed in Ar between Al_2O_3 platens at constant crosshead velocity, i.e. at nearly constant strain rate (CSR),[17] or under constant load (CL).[18] The temperature range was 1197–1400°C and the approximate stress range was 1–100 MPa. No appreciable reaction occurred between the specimens and the Al_2O_3 platens. A few crosshead velocities or loads were applied to each specimen at a given temperature to determine the value of the stress exponent n. Steady state was generally achieved within 2% strain after a strain-rate or stress change. The activation energy Q was determined from temperature changes during testing of single specimens at constant load. Specimens were deformed to total strains $< 10\%$.

Microstructures of selected deformed $ZrSiO_4$ specimens were examined by SEM of polished surfaces and TEM of ion-thinned foils.

Table 1
ICP-AES analysis of cation impurities in $ZrSiO_4$; estimated accuracy of ±20%

Element	Concentration (μg/g)
Al	700
Ba	35
Ca	370
Cu	26
Fe	350
Mg	31
Ti	450
Zn	24

3. Results and discussion

In all tests, clear steady states were obtained. In the CSR tests, the work-hardening rates were zero; in the CL tests, the strain rates were constant. Strain rate-vs.-stress data are shown in Fig. 3. The slight differences between the data points at ≈1400°C reflect experimental error, and probably a slight difference in grain size because the creep specimens were fabricated in different batches. When all of the data points were used to calculate the stress exponent, $n = 1.3 \pm 0.3$. When the data point at 1400°C and 1 MPa was excluded, $n = 1.1 \pm 0.1$. Thus, diffusional flow was the likely deformation mechanism.[14]

SEM and TEM observations were consistent with a diffusional mechanism. No damage was observed and the grain boundaries remained essentially free of glass (Fig. 4). Given the fine, equiaxed grains of the specimens,

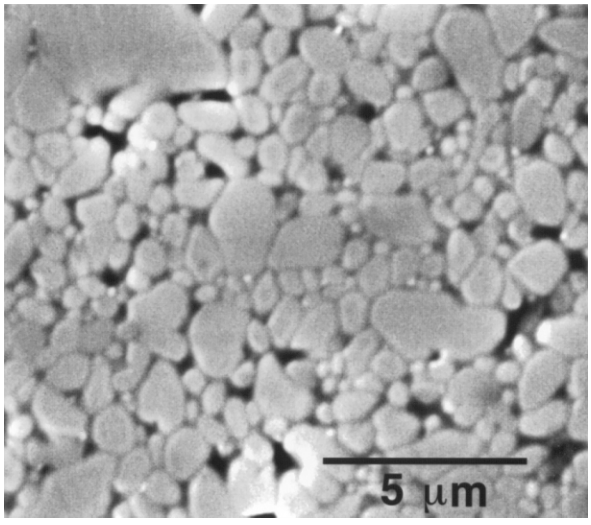

Fig. 1. SEM photomicrograph of heavily thermally etched $ZrSiO_4$ specimen.

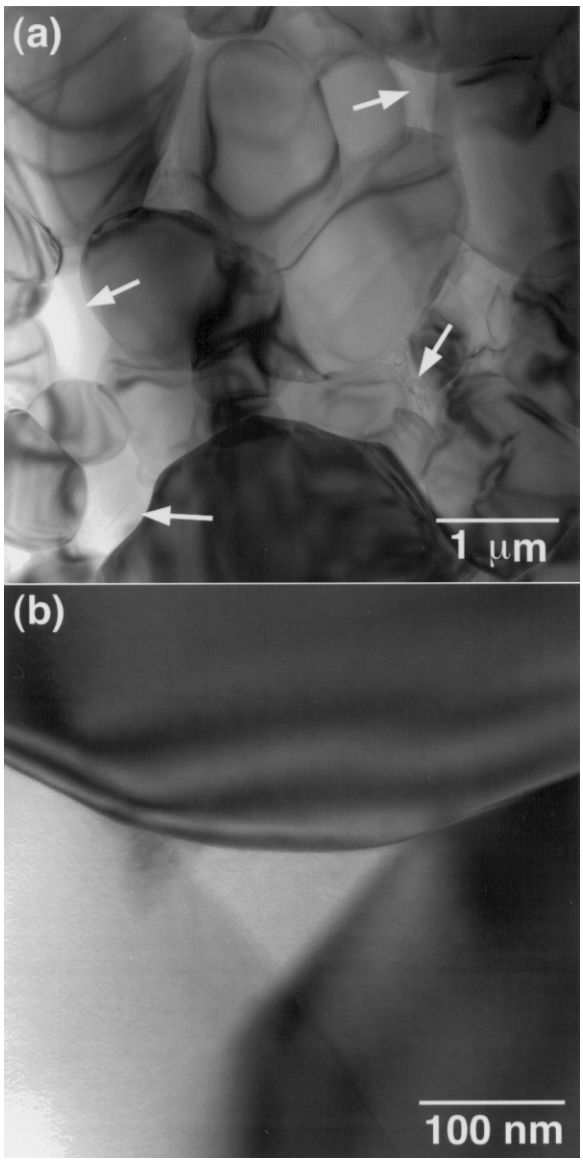

Fig. 2. TEM photomicrographs of as-sintered $ZrSiO_4$ specimen: (a) low-magnification view revealing grain-size distribution and presence of SiO_2-based glass (marked by arrows) and (b) higher-magnification view of glass at multiple-grain junction, but not along the adjoining grain boundaries.

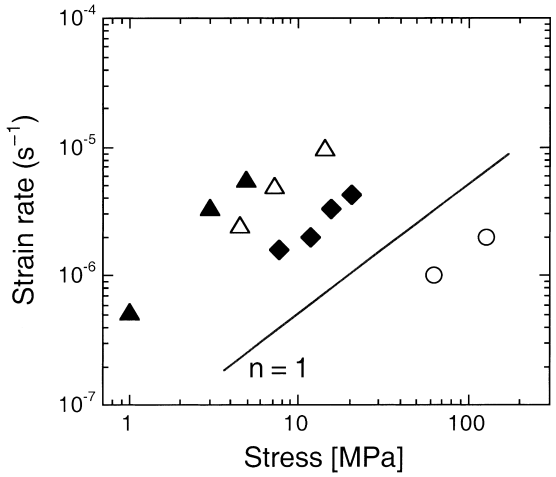

Fig. 3. Steady-state strain rate as a function of stress: open circles = 1197°C, CSR test; filled diamonds = 1300°C, CL test; open triangles = 1398°C, CSR test; filled triangles = 1400°C, CL test. Line drawn for $n = 1$.

grain-boundary sliding is the expected deformation mechanism.[14,19,20]

We believe that $n = 1.1 \pm 0.1$ is appropriate to describe the $ZrSiO_4$ deformation at stresses greater than ≈3 MPa. We have observed in recent tests of mullite[21] that $n = 1.0$ at stresses of > 10 MPa. At lower stresses near 1 MPa, values of n increased to ≈2. We believe that this change in n reflected a change in the deformation mechanism, perhaps related to the volume fraction of ceramic that was actually deforming. A detailed analysis of the phenomenon in mullite is being prepared for publication. We simply note that the limited data presented here agree with those of the more-comprehensive mullite study. In any case, whether or not one data point is excluded, the value of n for the $ZrSiO_4$ creep was, within experimental error, equal to 1.

The value of Q, calculated from two CL tests, was 470±40 kJ/mol (Fig. 5). The agreement between the two tests was excellent. This value is significantly lower than that estimated by Carbonneau et al. from flexural tests at lower temperatures, 625 kJ/mol.[12] Given that in these tests $n \approx 1$ and that no creep-induced damage was observed, the value of 470±40 kJ/mol appears to represent well creep of $ZrSiO_4$ at moderate stresses and temperatures greater than ≈1200°C.

Examination of known diffusion coefficients can allow identification of the rate-controlling diffusing species in creep. Because of its importance to geological studies,[22,23] a substantial body of diffusion data exists for $ZrSiO_4$.[24–27] Although neither Zr nor Si diffusion has been measured directly, O and Hf diffusion have been measured[25,26] and O and Zr diffusion have been modeled.[27] Shannon[28] has shown that the ionic radius of Hf^{+4} is almost identical to that of $Zr + 4$ in an octahedral coordination. Similar diffusion rates would, therefore, be likely for Hf and Zr.[26]

The agreement between the experimental diffusion coefficients[25,26] and those calculated theoretically[27] was satisfactory. O diffusion was found to have an activation energy of 448 kJ/mol;[25] Hf diffusion was found to have an activation energy of 812±54 kJ/mol.[26] From 1200–1400°C, the diffusion coefficients of O were 10^4–10^6 times faster than those of Hf.

Diffusion coefficients for the species that controls creep rates can be extracted from the $ZrSiO_4$ data of this study.[14,20,29] According to the Ashby–Verrall analysis,[20] for grain-boundary sliding accommodated by volume diffusion,

$$\dot{\varepsilon} = A(\sigma^n \Omega/kT)d^{-2}D_{\text{latt}}, \quad (1)$$

where $A = 98$, Ω is the molecular volume, k is Boltzmann's constant, T is the absolute temperature, d is the average grain size, and D_{latt} is the relevant diffusion coefficient. Data for $\dot{\varepsilon}$ and σ were taken from Fig. 5. The value of Ω was taken from the unit-cell data in Ref. 30. Calculated values of D_{latt} at 1197–1400°C are compared with literature diffusion values[25,26] in Fig. 6. The agreement between the creep diffusion coefficients and those for volume diffusion of O vacancies is excellent.

The rate-controlling species for creep should be the slowest-diffusing species moving along its fastest net path, not the fastest diffusing species. The finding that cation diffusion does not control creep, despite the likely higher activation energies of ≈800 kJ/mol and far slower diffusion rates at 1197–1400°C for Zr and, probably, Si,[26,27] must have resulted from an extrinsic effect. As shown in Table 1, the concentration of aliovalent cation impurities in the $ZrSiO_4$ specimens was >0.1%. The valences of these cations in an oxide would be primarily +2 or +3. Direct substitution into $ZrSiO_4$ lattice sites would therefore consume rather than generate cation vacancies. However, the crystal structure of $ZrSiO_4$ contains relatively large octahedral voids,[27,29] and it has been calculated that interstitial formation is energetically favorable in $ZrSiO_4$.[27,31]

Examples of incorporation into $ZrSiO_4$ of a representative +2 valence cation are shown below. In general, the cation can substitute either interstitially [Eq. (2)] or substitutionally [Eq. (3)].

$$4CaO \xrightarrow{ZrSiO_4} 4Ca_i^{\bullet\bullet} + V_{Zr}''''V_{Si}'''' + 4O_O^x; \quad (2)$$

$$V_{Zr}'''' + V_{Si}'''' + 4O_O^x + 4CaO \xrightarrow{ZrSiO_4} 2Ca_{Zr}'' + 2Ca_{Si}'' + 8O_O^x. \quad (3)$$

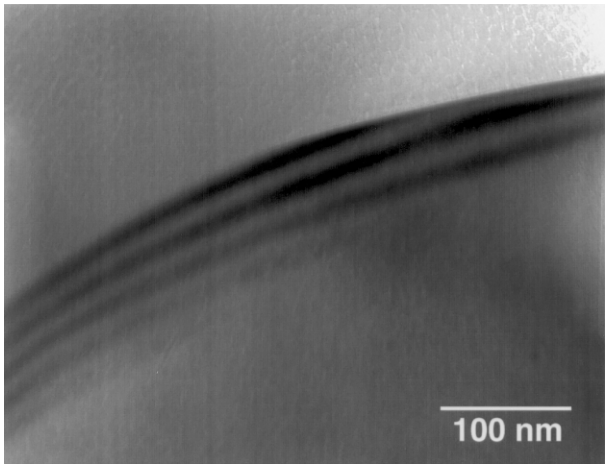

Fig. 4. TEM photomicrograph of typical grain boundary in a deformed $ZrSiO_4$ specimen.

Although no proof can be offered, the agreement between diffusion coefficients calculated from creep and those of oxygen vacancy diffusion can be rationalized as follows. Presence of charged cation interstitials could induce a net increase in Zr and Si vacancy concentrations to preserve electroneutrality; i.e. Eq. (2) dominates Eq. (3). Schottky equilibrium would then dictate a corresponding decrease in the O vacancy concentration with increases in cation vacancy concentrations:

$$\text{null} \longrightarrow V_{Zr}'''' + V_{Si}'''' + 4V_O^{\bullet\bullet}; \quad (4)$$

$$K_S = [V_{Zr}''''][V_{Si}''''][V_O^{\bullet\bullet}]^4. \quad (5)$$

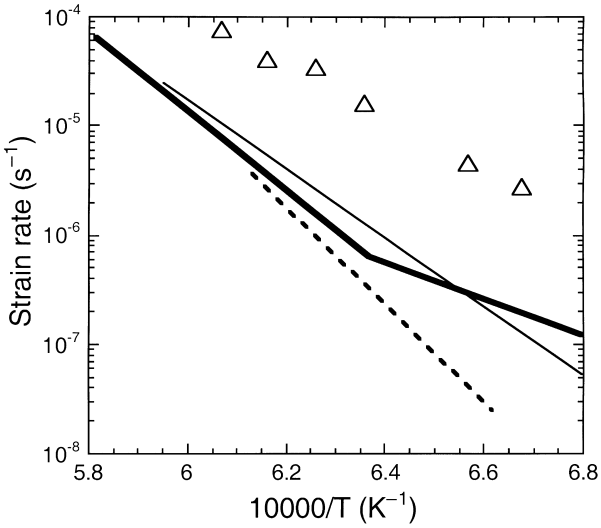

Fig. 5. Steady-state strain rate vs. reciprocal temperature in CL tests for stresses of 3 MPa (open triangles) and 20 MPa (filled triangles).

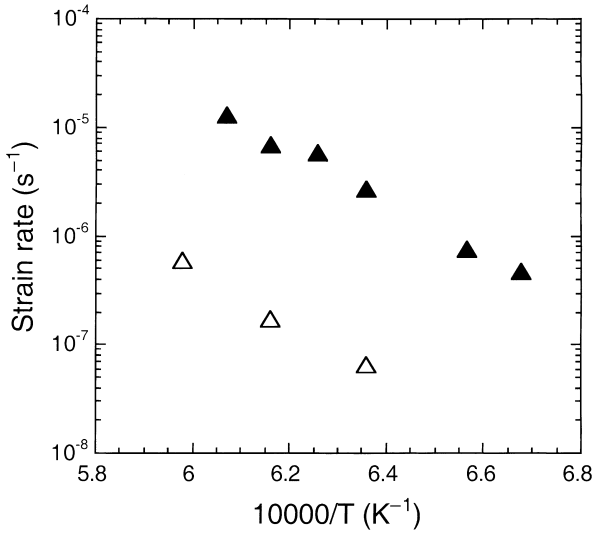

Fig. 6. Values of D_{latt} calculated from creep data (solid line) and literature values for O diffusion[25] (dashed line) and Hf diffusion[26] (bold line) in $ZrSiO_4$.

Formation and migration of O vacancies, which has an activation energy of ≈450 kJ/mol,[25] would therefore control creep rates if the majority of aliovalent cation impurities entered the $ZrSiO_4$ lattice interstitially. It has been calculated that Zr vacancy migration in $ZrSiO_4$ has an activation energy of only ≈100 kJ/mol.[27] If one assumes that Si vacancies have similar migration energies (there is no obvious competing assumption to make), O diffusion must have controlled the creep rates in this study because of the aliovalent cation impurities present in the $ZrSiO_4$ specimens. It is further noted that intrinsic vacancy concentrations, estimated from [V]∼exp−(Q/RT), are orders of magnitude lower at 1197–1400°C than the total concentration of aliovalent impurities in the $ZrSiO_4$ specimens.

It is also possible that grain-boundary diffusion of a cation could have controlled the creep rates.[14] There is, however, no evidence to support this possibility. The rather high total concentration of aliovalent cation impurities and the remarkable agreement of the creep diffusion coefficients with those of oxygen diffusion militate strongly against that possibility.

Comparison of activation energies and creep rates of $ZrSiO_4$ with those of mullite, which is another candidate matrix for ceramic composites, is also useful in interpreting the data. Although substantial scatter exists, with values ranging from ≈360 to 1050 kJ/mol for diffusional creep of mullite, there is a broad trend for Q to be higher in specimens in which substantial glass was present. The average value of Q for crystalline mullite is ≈700 kJ/mol.[31–38]. With respect to $ZrSiO_4$ creep data, the difference between Q of 470 or 625 kJ/mol may either be related to differences in specimen glass content or to the fact that the higher value from the flexural test was only approximate because of concomitant occurrence of creep and cavitation.

Carbonneau et al. previously compared creep of $ZrSiO_4$ with that of mullite and found that mullite was approximately two orders of magnitude more creep-resistant.[13] However, those results were doubtless dominated by the presence of a glass phase. There are several reports in the literature for creep of mullite that is highly phase-pure. In three studies, the specimens were >90% dense and exhibited grain sizes of ≈1.5 μm.[33,34,38] Representative mullite data taken at a steady-state stress of 100 MPa can, therefore, be compared with $ZrSiO_4$ data taken at 20 MPa by extrapolating the $ZrSiO_4$ data to 100 MPa. To do so, the $\dot{\varepsilon}$ values for $ZrSiO_4$ were increased by a factor of $(\Delta\sigma)^{1.1}$, i.e., by a factor of 5.87, and then plotted against those of mullite (Fig. 7). For highly crystalline specimens at 1200–1400°C, mullite is approximately one order of magnitude more creep-resistant than the $ZrSiO_4$ used in this study. This result qualitatively agrees with the conclusions of Carbonneau et al. and suggests that mullite is likely to be superior to commercial-grade $ZrSiO_4$ as a ceramic or composite matrix in many elevated-temperature structural applications. If, however, highly pure bulk $ZrSiO_4$ material can be fabricated, perhaps its diffusional creep resistance can be improved substantially because diffusion of Zr or Si may then control creep rates.

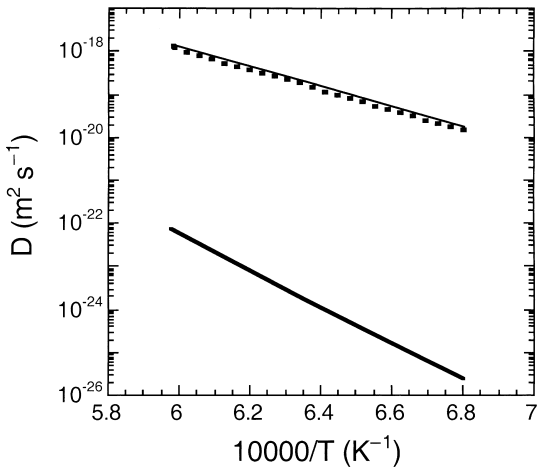

Fig. 7. Calculated creep rates at 100 MPa stress for $ZrSiO_4$ (triangles) and creep rates for mullite from Torrecillas et al.[34] (bold line), Hynes and Doremus35 (fine line), and Tkalcec et al.[39] (dashed line); $ZrSiO_4$ data extrapolated from $\sigma = 20$ MPa.

4. Conclusions

$ZrSiO_4$ ceramics were compressed in Ar at 1197–1400°C. For stresses of ≈3–120 MPa, creep occurred by diffusional flow, with the likely mechanism being grain-boundary sliding. Electron microscopy revealed no deformation-induced change in the microstructures of any of the specimens, which is consistent with creep by grain-boundary sliding. Comparison with published values indicated that creep was controlled by diffusion of O vacancies. The stress exponent was 1.1±0.1 and the activation energy for creep was 470±40 kJ/mol. At 1400°C and 1 MPa, there was an indication of an increase in the value of n.

Acknowledgements

We thank B. J. Polzin and R. N. Tsaliagos for help with specimen preparation and Profs. R. N. Singh and E. B. Watson for helpful discussions. This work was supported at Argonne National Laboratory by the Defense Advanced Research Projects Agency, through a Department of Energy Interagency Agreement, under Contract W-31-109-Eng-38, and at the University of Sevilla by IBERDROLA and the Spanish Ministerio de Educación, CICYT Project MAT97-0562-C02-01.

References

1. Brezny, B. and Engel, R., Evaluation of zircon brick for steel ladle slag lines. *Am. Ceram. Soc. Bull.*, 1984, **63**, 880–883.
2. Gardner, R. A. and Buchanan, R. C., High temperature loss of silica from zircon and refractory silicates. *J. Electrochem. Soc.*, 1975, **122**, 205–211.
3. Ewing, R. C., Lutze, W. and Weber, W. J., Zircon: a host-phase for the disposal of weapons plutonium. *J. Mater. Res.*, 1995, **10**, 243–246.
4. Curtis, C. E. and Sowman, H. G., Investigation of the thermal dissociation, reassociation, and synthesis of zircon. *J. Am. Ceram. Soc.*, 1953, **36**, 190–198.
5. Butterman, W. C. and Foster, W. R., Zircon stability and the ZrO_2–SiO_2 phase diagram. *Am. Mineral.*, 1967, **52**, 880–885.
6. Kanno, Y., Thermodynamic and crystallographic discussion of the formation and dissociation of zircon. *J. Mater. Sci.*, 1989, **24**, 2415–2420.
7. Singh, R. N., High-temperature mechanical properties of a uniaxially reinforced zircon-silicon carbide composite. *J. Am. Ceram. Soc.*, 1990, **73**, 2399–2406.
8. Singh, R. N., Mechanical properties of a zircon matrix composite reinforced with silicon carbide whiskers and filaments. *J. Mater. Sci.*, 1991, **26**, 1839–1846.
9. Mori, T., Yamamura, H., Kobayashi, H. and Mitamura, T., Preparation of high-purity $ZrSiO_4$ powder using sol-gel processing and mechanical properties of the sintered body. *J. Am. Ceram. Soc.*, 1992, **75**, 2420–2426.
10. Shi, Y., Huang, X. and Yan, D., Mechanical properties and toughening behavior of particulate-reinforced zircon matrix composites. *J. Mater. Sci. Lett.*, 1999, **18**, 213–216.
11. Polzin, B. J., Cruse, T. A., Houston, R. L., Picciolo, J. J., Singh, D. and Goretta, K. C., Fabrication and characterization of oxide fibrous monoliths produced by coextrusion. *Ceram. Trans.*, 2000, **103**, 237–244.
12. Carbonneau, X., Hamidouche, M., Olagnon, C., Fantozzi, G. and Torrecillas, R., High temperature behaviour of a zircon ceramic. *Key Eng. Mater.*, 1997, **132-136**, 571–574.
13. Carbonneau, X., Olagnon, C. and Fantozzi, G., Creep and crack growth of zircon and mullite based materials. *Key Eng. Mater.*, 1999, **161-163**, 627–630.
14. Cannon, W. R. and Langdon, T. G., Review: creep of ceramics. *J. Mater. Sci.*, 1983, **18**, 1–50.
15. Raj, R. and Morgan, P. E. D., Activation energies for densification, creep, and grain-boundary sliding in nitrogen ceramics. *J. Am. Ceram. Soc.*, 1981, **64**, C143–C145.
16. ASTM Standard E 112-88, Standard test methods for determining average grain size. *Am. Soc. Test. Mater.*, Philadelphia, 1992, pp. 294–319.
17. Routbort, J. L., Work hardening and creep of MgO. *Acta Metall.*, 1979, **27**, 649–661.
18. de Arellano-Lopez, A. R., Dominguez-Rodriguez, A., Goretta, K. C. and Routbort, J. L., Plastic deformation mechanisms in SiC-whisker-reinforced Al_2O_3. *J. Am. Ceram. Soc.*, 1993, **76**, 1425–1432.
19. Raj, R. and Ashby, M. F., On grain boundary sliding and diffusional creep. *Metall. Trans.*, 1971, **2**, 1113–1127.
20. Ashby, M. F. and Verrall, R. A., Diffusion-accommodated flow and superplasticity. *Acta Metall.*, 1973, **21**, 149–163.
21. de Arellano-Lopez, A. R., unpublished information, 2001.
22. Watson, E. B. and Harrison, T. M., Zircon saturation revisited: temperature and composition effects in a variety of crustal magma types. *Earth Planet. Sci. Lett.*, 1983, **64**, 295–304.
23. Chen, Y. D. and Williams, I. S., Zircon inheritance in mafic inclusions from Bega Bayholith granites, southeastern Australia: an ion microprobe study. *J. Geophys. Res.*, 1990, **95**, 17787–17796.
24. Cherniak, D. J., Hanchar, J. M. and Watson, E. B., Rare earth diffusion in zircon. *Chem. Geol.*, 1996, **136**, 289–301.
25. Watson, E. B. and Cherniak, D. J., Oxygen diffusion in zircon. *Earth Planet. Sci. Lett.*, 1997, **148**, 527–544.
26. Cherniak, D. J., Hanchar, J. M. and Watson, E. B., Diffusion of tetravalent cations in zircon. *Contrib. Mineral. Petrol.*, 1997, **127**, 383–390.
27. Williford, R. E., Weber, W. J., Devanathan, R. and Cormack, A. N., Native vacancy migrations in zircon. *J. Nucl. Mater.*, 1999, **273**, 164–170.
28. Shannon, R. D., Revised effective ionic radii and systematic studies of interatomic distances in halides and chalcogenides. *Acta Cryst.*, 1976, **A32**, 751–767.
29. Jimenez-Melendo, M., de Arellano-Lopez, A. R., Dominguez-Rodriguez, A., Goretta, K. C. and Routbort, J. L., Diffusion-controlled plastic deformation of $YBa_2Cu_3O_x$. *Acta Metall. Mater.*, 1995, **43**, 2429–2434.
30. Ramakrishnan, S. S., Gokhale, K. V. G. K. and Subbarao, E. C., Solid solubility in the system zircon-hafnon. *Mater. Res. Bull.*, 1969, **4**, 323–327.
31. He, Y. and Cormack, A. N., Alfred University, NY, unpublished information (2000).
32. Penty, R. A. and Hasselman, D. P. H., Creep kinetics of high-purity, ultra-fine grain polycrystalline mullite. *Mater. Res. Bull.*, 1972, **7**, 1117–1124.
33. Lessing, P. A., Gordon, R. S. and Mazdiyasni, K. S., Creep of polycrystalline mullite. *J. Am. Ceram. Soc.*, 1975, **58**, 149–150.
34. Torrecillas, R., Fantozzi, G., de Aza, S. and Moya, J. S., Thermomechanical behaviour of mullite. *Acta Mater.*, 1997, **45**, 897–906.
35. Hynes, A. P. and Doremus, R. H., High-temperature compressive creep of polycrystalline mullite. *J. Am. Ceram. Soc.*, 1991, **74**, 2469–2475.
36. Nixon, R. D., Chevacharoenkul, S., Davis, R. F. and Tiegs, T. N., Creep of hot-pressed SiC whisker reinforced mullite. *Ceram. Trans.*, 1990, **6**, 579–603.
37. Torrecillas, R., Calderon-Moreno, J. M., Moya, J. S., Reece, M. J., Davies, C. K. L., Olagnon, C. and Fantozzi, G., Suitability of mullite for high temperature applications. *J. Eur. Ceram. Soc.*, 1999, **19**, 2519–2527.
38. Ohira, H., Shiga, H., Ismail, M. G. M. U., Nakai, Z., Akiba, T. and Yasuda, E., Compressive creep of mullite ceramics. *J. Mater. Sci. Lett.*, 1991, **10**, 847–849.
39. Tkalcec, E., Nass, R., Krajewski, T., Rein, R. and Schmidt, H., Microstructure and mechanical properties of slip cast sol-gel derived mullite ceramics. *J. Eur. Ceram. Soc.*, 1998, **18**, 1089–1099.